HEWLETT-PACKARD JOURNAL

TECHNICAL INFORMATION FROM THE -hp- LABORATORIES

CORPORATE OFFICES • 1501 PAGE MILL ROAD • PALO ALTO, CALIFORNIA 94304 • VOL. 17, NO. 8 APRIL, 1966

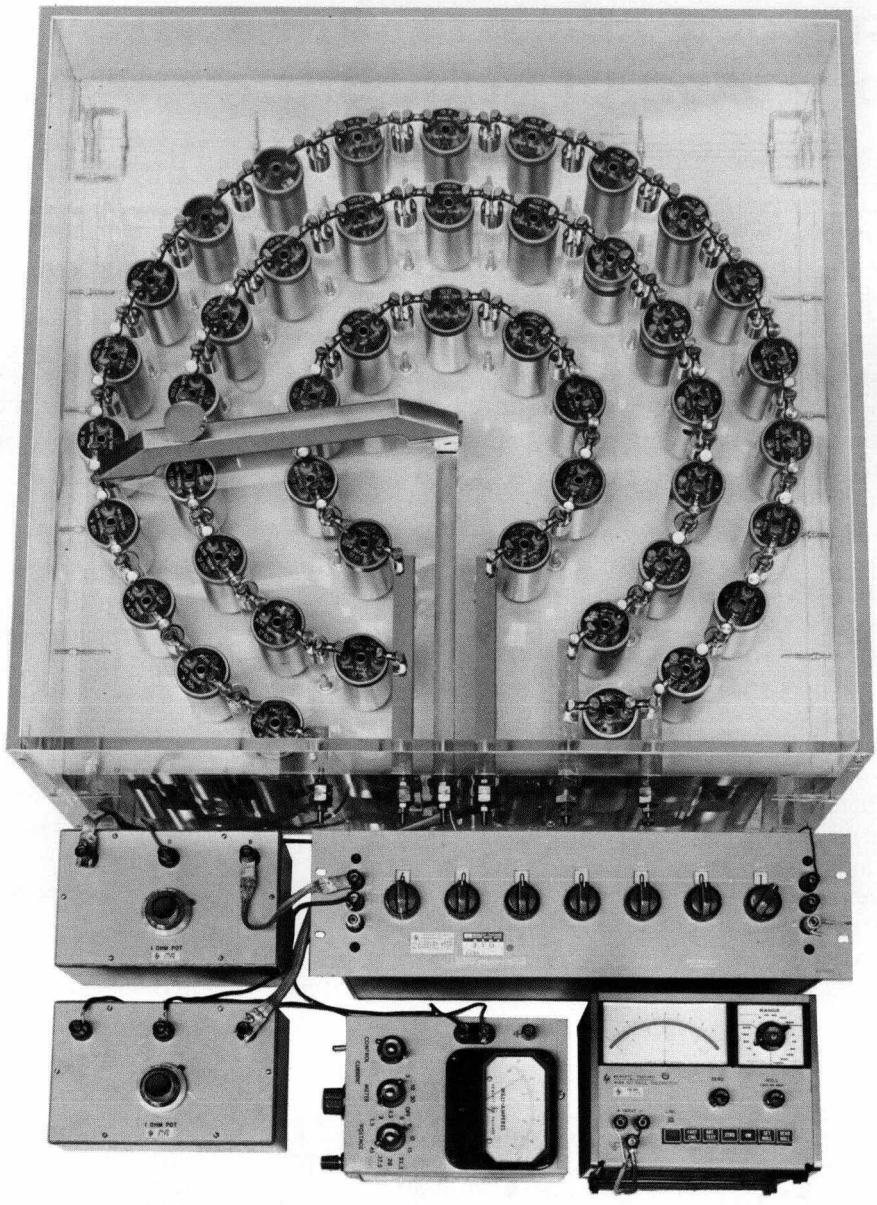

COVER: 1.5 X 10^{-8} ACCURACY DC VOLTAGE DIVIDER USING NEW -hp- STANDARD RESISTORS, p. 8

SEE ALSO: AUTOMATIC-NULLING DISTORTION ANALYZER, p. 2

EMITTER-FOLLOWER STABILITY, p. 16

PRINTED IN U. S. A.

A NEW DISTORTION ANALYZER WITH AUTOMATIC NULLING AND BROADENED MEASUREMENT CAPABILITY

A new audio-RF distortion analyzer has been designed which, when roughly pre-tuned, tracks the signal to be measured and automatically nulls the fundamental frequency. More consistent measurements are thus obtained — and over a wider frequency range.

THE TOTAL HARMONIC DISTORTION METHOD of analyzing the effects of system non-linearity has been popular for a number of years because of the speed and simplicity of the equipment needed for making the measurement. The method is now even more attractive as a result of recent developments that permit the signal-filtering part of the measurement to be performed automatically.

A new 5 Hz-to-600 kHz distortion analyzer has been designed with circuits that automatically tune the rejection filter to suppress the fundamental of the input signal while the remaining signal components are measured. The operator need only tune the filter approximately to the null, then switch to the automatic mode whereupon the instrument seeks the true null and retains it. Distortion measurements that formerly required patience and considerable skill, because of the sharpness of the rejection filter, may now be performed without requiring a high degree of operator training. Besides simplifying distortion measurements, automatic nulling also assures accuracy and repeatability, especially if the test signal tends to drift.

In addition to automatic nulling, the new Distortion Analyzer has other refinements made possible by new solid-state devices. As a result, overall performance of the new analyzer is greatly improved with respect to its vacuum-tube predecessors. Distortion levels lower than 0.03% are easily resolved since the most sensitive range of the distortion measuring circuits is 0.1% full scale (300 μV) and the noise level is less than 25 μV rms.

The rejection filter tuning range has been increased considerably beyond the audio range in the new instrument, the full range now being 5 Hz to 600 kHz. In addition, the voltage-measuring frequency range has been extended up to 3 MHz (Fig. 2), enabling measurement of frequency components as high as the fifth harmonic of 600 kHz signals.

To reduce interference from power-line hum, if present in the signal being measured, the Analyzer has a switchable high-pass filter for use with input signals higher than 1 kHz. The filter attenuates 60-Hz power-line interference by more than 40 dB. Rear panel terminals permit operation from bat-

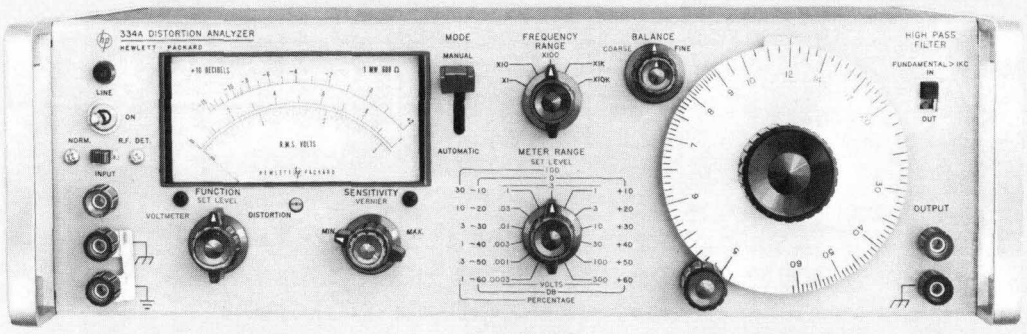

Fig. 1. *Model 334A Distortion Analyzer has higher sensitivity and broader bandwidth than vacuum-tube predecessors. Instrument reads distortion directly in percent of total signal or in decibels below total signal level. Higher sensitivity of new Analyzer allows 'Set Level' (100% or 0 dB) to be placed on 0.3-V voltmeter range (10 dB thus must be added to readings when instrument is used as dB meter in 'Voltmeter' mode).*

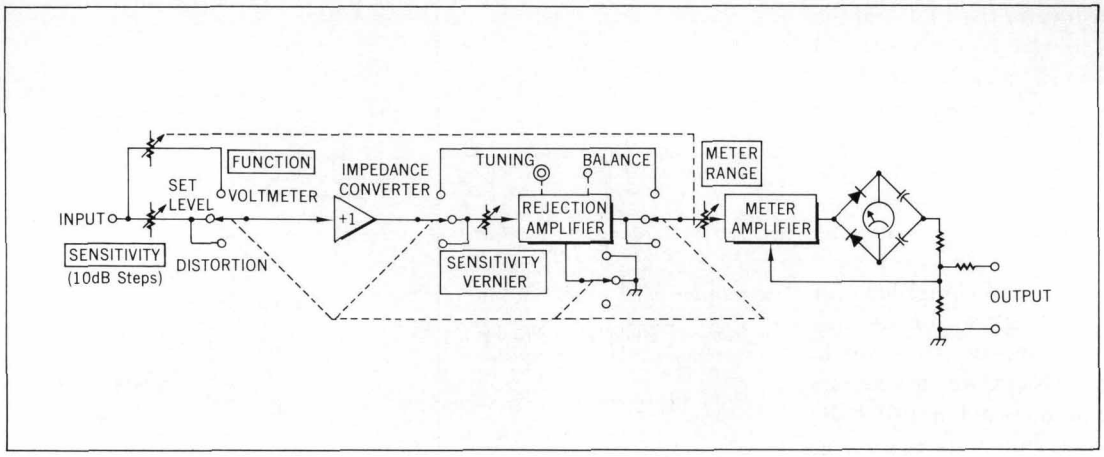

Fig. 3. *Elements of Distortion Analyzer. Instrument functions as broadband calibrated ac voltmeter in 'Voltmeter' mode and as signal level indicator in 'Set Level' mode. In 'Distortion' mode, Rejection Amplifier can be tuned to suppress fundamental frequency of input signal, permitting comparison of distortion components level to total signal level.*

teries should it be desired to eliminate ground loops arising from power line interconnects.

The new instrument also has an RF detector to enable distortion measurements of the modulating waveform on the carrier of AM radio transmitters. A meter with VU ballistic characteristics has been designed for use with analyzers that are to be used for performance checks conforming to FCC regulations.

CIRCUIT ARRANGEMENTS

The basic design of the new Distortion Analyzer essentially follows ac voltmeter practice in that there is a low-noise impedance converter at the input, followed by an attenuator, a broadband amplifier, an ac-to-dc converter, and a meter, as shown in the block diagram of Fig. 3. The tunable rejection amplifier is switched in or out as required.

The impedance converter uses a field-effect transistor (FET) to obtain exceptionally high input impedance and a noise level that is less than 25 μV referred to the input (with input shorted). The FET input circuit is bootstrapped to insure that the input impedance has high linearity and that the gain at the input of the converter is independent of source impedance.

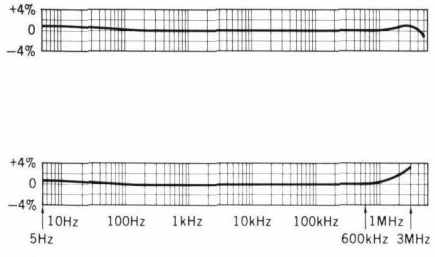

Fig. 2. *Typical frequency response of new Distortion Analyzer. Upper curve shows response of meter to constant amplitude input signal with Distortion Analyzer in 'Voltmeter' mode. Response is within 2% (0.2 dB) throughout 5 Hz-3 MHz range. Lower curve is with instrument in 'Set Level' mode. As shown, response is flat considerably beyond 5 Hz-600 kHz rejection filter tuning range.*

TOTAL HARMONIC DISTORTION MEASUREMENTS

Total harmonic distortion (THD) measurements are made by applying a sine wave signal of high purity to the input of a system under test while the distortion analyzer measures the system output. A tunable notch filter in the analyzer suppresses the signal fundamental, leaving the distortion components to be measured by the analyzer's voltmeter circuits. The ratio of the measured distortion components to the total signal output, including fundamental, is defined as the distortion and can be read directly on the meter.

The method is fast in that it is only necessary to establish a reference level with the filter switched out, and to then make a reading with the filter, tuned to reject the fundamental, in the circuit. The measurement may be made quickly at several frequencies within the passband of interest, one of the major advantages of the THD method.

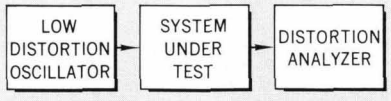

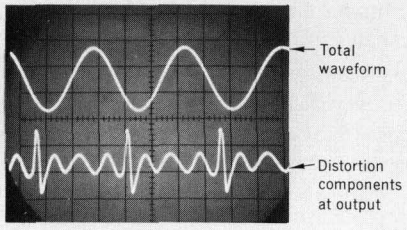

Viewing the distortion products presented at the distortion analyzer output terminals can also provide considerable supplementary information about system performance (see photo above). Small oscillations or discontinuities that may not be noticeable on the total waveform are seen on the oscilloscope display of the residuals. Noise, hum, and other nonharmonically related interference can also be identified.

Distortion analyzers also provide other information about the performance of a system. Gain or loss, frequency response, and noise may be measured, using the instrument as a broadband ac voltmeter, at the same time that distortion measurements are made.

The load resistors for the FET and the second stage are also bootstrapped, all within an overall negative feedback loop to achieve high loop gain and therefore high linearity for the impedance converter transfer characteristic. This insures that the converter introduces negligible distortion into the signal.

The broadband meter amplifier also uses a large feedback factor for linearity and gain stability. The ac-to-dc converter circuit is of the type wherein each diode conducts for a full half-cycle. The meter thus responds to the average value of the waveform but it is calibrated to read the rms value of a sine wave. Ordinarily, any difference that may exist between the average-responding meter indication and the true rms value is small[1] and of little concern since the majority of distortion measurements are of a relative nature. If the true rms value of the residual waveform is desired, however, it is readily found by connecting an rms-responding meter to the OUTPUT terminals of the analyzer.

The OUTPUT terminals supply a voltage that is proportional to the current supplied to the meter rectifiers. The output is taken from the calibration network in the feedback circuit of the meter amplifier and thus, at frequencies up to 600 kHz, the output waveform is not subject to the diode crossover distortion that has been characteristic of earlier average-responding circuits. Maximum output, corresponding to full-scale meter deflection is 0.1 V rms.

[1] Bernard M. Oliver, 'Some Effects of Waveform on VTVM Readings,' **'Hewlett-Packard Journal,'** Vol. 6, Nos. 8, 9, and 10, April-May, 1955.

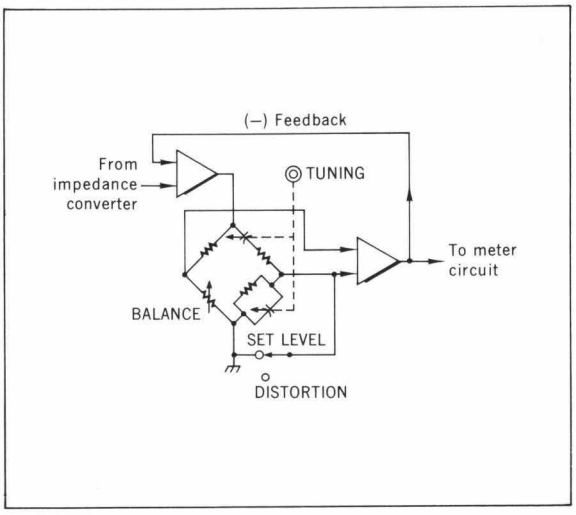

Fig. 4. *Rejection amplifier has Wien bridge in interstage coupling network to suppress fundamental of input signal when instrument is in 'Distortion' mode. In 'Set Level' mode, one corner of bridge is grounded and signal is coupled through with no frequency rejection. Feedback flattens response of total amplifier.*

REJECTION AMPLIFIER

During a distortion measurement, the fundamental component of the signal is rejected by the tunable Wien bridge in the interstage coupling network of the rejection amplifier (Fig. 4). To prevent attenuation of harmonics, the distortion analyzer uses heavy feedback around the rejection amplifier to flatten the overall response, except in the deepest part of the notch where the Wien bridge attenuation is greater than available amplifier gain. With feedback, sharpness of the null is increased, as shown by the dotted line in Fig. 5. The notch width is only 0.007% of the center frequency at the —70-dB points and the second harmonic is attenuated typically less than 0.2 dB within a fundamental range of 20 Hz to 20 kHz, while the fundamental is attenuated more than 80 dB.

AUTOMATIC NULLING CIRCUITRY

The automatic nulling system is based on the phase characteristics of the Wien bridge, plotted as the dashed line in Fig. 5. As shown, the phase of the residual signal across the corners of the bridge lags the driving signal by 90°, if the bridge is tuned slightly below the signal frequency, and leads by 90° if the bridge is tuned above. A phase-sensitive detector therefore is able to sense any mistuning and indicate the direction that a correction should take.

Similarly, unbalance in the resistive arm of the bridge results in an output signal that is either in phase or 180° out of phase with the driving signal, depending upon the direction of unbalance. Thus, two phase-sensitive detectors, one with the reference signal phase-shifted 90°, are able to separate the effects of unbalance in both the resistive and reactive arms, and to provide information for readjustment.

Automatic readjustment is provided by photoconductors in the arms of the bridge, as shown in the diagram of Fig. 6. The photoconductors in the reactive arm are illuminated by lamps controlled by the quadrature phase-sensitive detector. The photoconductor in the resistive arm is illuminated by a lamp controlled by the in-phase detector. The outputs of the phase detectors thus adjust the resistance of the photoconductors by means of the lamps to bring the bridge into balance.

The circuits are able to track frequency deviations of at least 1%. Typical instrument response time is on the order of 5 seconds for a 1% step change in frequency, assuring no delay in the

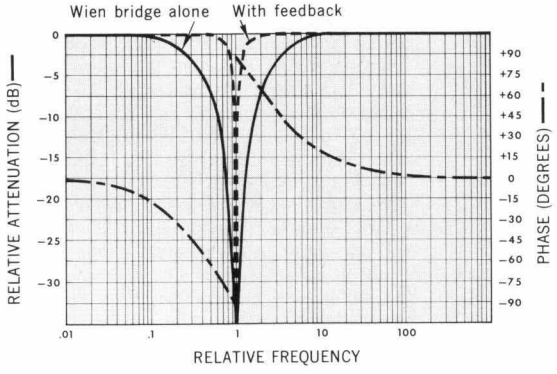

Fig. 5. *Frequency response characteristics across corners of Wien bridge with and without overall amplifier feedback. Diagram also shows phase plot, which has discontinuity from +90° to −90° at center of rejection notch.*

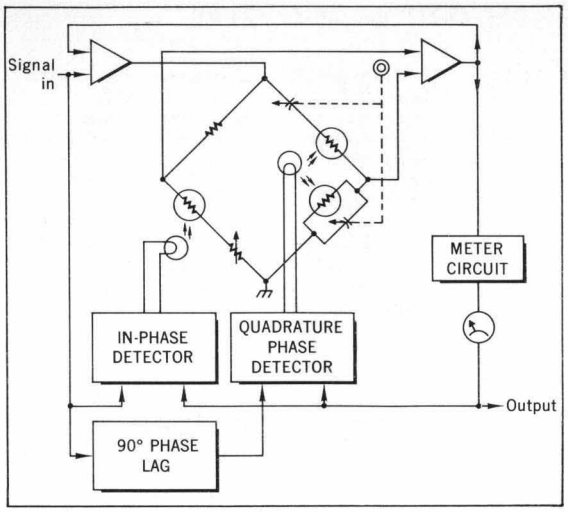

Fig. 6. *Rejection amplifier with automatic nulling circuitry. Phase detectors sense bridge unbalance and control intensity of lamps to change resistance of photoconductors, thus adjusting bridge to reject fundamental frequency of input signal.*

measurement if the frequency should vary.

The bridge is self-compensating as far as temperature changes are concerned. The servo action of the automatic nulling circuitry maintains the null at all times, even though photoconductors tend to drift with changes in temperature.

READING DIFFERENCES

Automatic nulling greatly simplifies using a distortion analyzer and makes certain that the null is retained, assuring accuracy and repeatability. Automatic nulling also is less subject to certain tuning errors. For instance, experience has shown that there may be slight differences between the null obtained by manual tuning and that obtained by use of the 'Automatic' mode. This can occur if the phase of the harmonics is such that a small amount of fundamental *reduces* the total area of the residual waveform. Slight manual mistuning of the rejection amplifier may thus result in an artificially low null. On the other hand the phase detectors of the automatic nulling system respond primarily to the magnitude of the fundamental and do not attempt to minimize the total waveform passed to the metering circuit. Hence, automatic nulling is less subject to this type of error.

The phase detectors are gated by a square wave derived from the fundamental and are thus somewhat sensitive to the phase of odd signal harmonics. This can lead to errors although the errors are relatively small compared to those that arise from slight mistuning of a manually-controlled instrument. The errors that can result from the phase of the odd harmonics are plotted in Fig. 7, which shows maximum errors to be less than 2 dB. A null reading that is 2 dB high, when the true null is 62 dB, is the same as the difference between 0.1% distortion and 0.08%. Typically, the largest reading

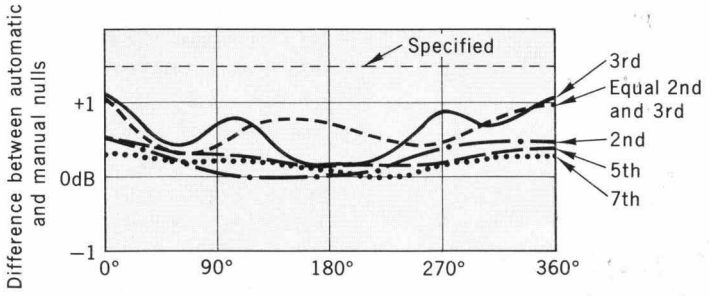

Fig. 7. *Possible differences between manual and automatic nulling depth resulting from phase displacement of odd harmonics. Majority of differences are less than 1 dB and in practice, seldom exceed ½ dB.*

DESIGN LEADERS

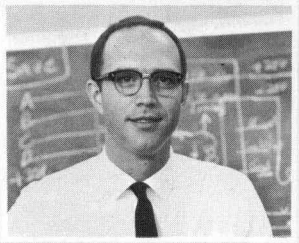

CHARLES R. MOORE

Dick Moore graduated from Princeton University in 1956 with a BS degree in Geological Engineering and then spent two years in the Army as a communications section chief. On completing his Army service, he worked for two years in automatic control sensors and then entered the University of California. After obtaining a MSEE degree in 1961, Dick joined Hewlett-Packard where he worked on the –hp– Model 716B Klystron Power Supply and as Group Leader on the 400E and 400F AC Voltmeters and on the 331A-334A Distortion Analyzers.

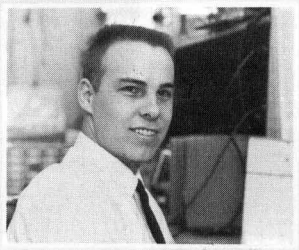

TERRY E. TUTTLE

Terry Tuttle joined Hewlett-Packard in 1962 after earning his BSEE degree from Utah State University. At –hp–, Terry has worked on the 331A-334A Distortion Analyzers and as Design Leader on the soon-to-be-announced Model 400F highly-sensitive AC Voltmeter. He is a member of Phi Kappa Phi honorary fraternity and at present is earning a Master's degree in EE under the –hp– Honors Cooperative Program.

LARRY A. WHATLEY

Larry Whatley joined Hewlett-Packard in 1964 where he has been concerned primarily with the –hp– Models 331A-334A Distortion Analyzers. Prior to that time, he worked in space instrumentation for a year with an aerospace firm. Larry graduated from Oklahoma State University with a BSEE degree in 1962 and obtained an MS degree there in General Engineering in 1963.

A FAMILY OF DISTORTION ANALYZERS

Distortion Analyzer described in accompanying article is one of four new analyzers which all use same measuring circuitry with wide filter tuning range (5 Hz to 600 kHz)

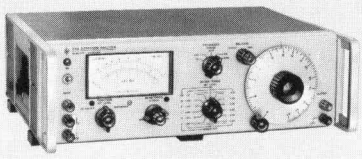

and broad voltmeter frequency range (up to 3 MHz).

For applications where lower initial cost is more important than speed and convenience of automatic nulling, Models 331A (photo) and 332A have precision mechanical drives for accurate manual tuning without automatic nulling (switched high-pass filter is also omitted). Model 332A has RF detector but Model 331A does not.

Model 333A is identical to Model 334A Automatic Nulling Distortion Analyzer except that RF detector is omitted.

difference that has been noted in practice is ½ dB.

LINEARITY

The overall performance of the new analyzer has been evaluated by using a wave analyzer to measure the distortion that a typical Distortion Analyzer introduces into a signal. For these tests, a signal with distortion products at least 100 dB below the fundamental was applied to the Distortion Analyzer input. When the test signal was set to 5 kHz, 0.3V rms (100% 'Set Level'), the wave analyzer showed the Distortion Analyzer output to have a 2nd harmonic (10 kHz) level 84 dB below the fundamental.* The 3rd harmonic (15 kHz) was —100 dB. By contrast, any indication of total distortion lower than —76 dB is off the scale of the Distortion Analyzer and within the noise level. Hence, distortion introduced by the Distortion Analyzer in the audio range is so low as to not be distinguishable from the noise level.

With a 500-kHz input, the wave analyzer indicated a 2nd harmonic (1 MHz) level of — 78 dB and a 3rd harmonic (1.5 MHz) of — 70 dB showing that even at 500 kHz, harmonics introduced by the distortion analyzer are of very low order. The distortion analyzer reading in this case was — 71 dB.

WAVE ANALYZER PRE-AMP

Similar measurements confirmed that whenever a Distortion Analyzer is to be used as a filter pre-amplifier for a wave analyzer in the measurement of very low distortion signals, it should be operated at the lowest possible signal level. This agrees with the theory that when the signal level changes in a system that is not absolutely linear, the amplitude of the harmonics varies at a greater rate than the fundamental.[2]

To obtain quantitative information about the relation of harmonics to signal level, the Distortion Analyzer SENSITIVITY VERNIER control, which follows the Impedance Converter, was set to the maximum position, thus allowing minimum signal input to the Impedance Converter. With a 0.3-volt (100% 'Set Level'), 5-kHz input, the 2nd harmonic in the Distortion Analyzer output measured 84 dB below the fundamental. When the input signal level was changed to 0.1 V (30% 'Set Level'), the 2nd harmonic measured —91 dB with respect to the fundamental, a relative improvement of 7 dB and a total change of 17 dB with respect to the original 0.3-V input level. Since theory showed that the 2nd harmonic would change 20 dB for each 10 dB change in signal level, one would expect a net change of 10 dB with respect to the new signal level. The measurement did not quite conform to this rate of change because two independent circuits were involved, the Impedance Converter and the Rejection Amplifier.

Measurement of the 3rd harmonic showed a level of —100 dB with respect to the 0.3-volt 5-kHz input signal, and —110 dB with respect to the 0.1-volt input. Theory indicated a 20–dB improvement but the actual change was —10 dB, again for the same reason. Nevertheless, these measurements showed that the performance of a distortion analyzer can be enhanced by setting the 'Set Level' reference at values lower than 100%.

* In these measurements, the range of the wave analyzer reading was increased 60 dB by setting the Distortion Analyzer meter range switch for highest sensitivity with the fundamental nulled out, which maximizes the residual signal at the output.

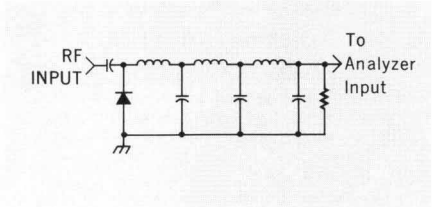

Fig. 8. *RF detector is untuned and responds to signals within range of 550 kHz to 65 MHz. Demodulated signals are attenuated above 100 kHz to prevent RF carrier feed-through.*

RF DETECTOR

The broadband RF detector in the new analyzer is untuned and accepts RF signals greater than 1 volt within a range of 550 kHz to 65 MHz. In the broadcast band (550–1600 kHz), the detector introduces less than 0.3% distortion into signals carried on 3–8 V rms carriers modulated 30% (see Table I). The ac input impedance of this detector is summarized in Table II.

A schematic of the RF detector is shown in Fig. 8. The filter, a 6-pole Butterworth type, cuts off above 100 kHz, allowing the 5th harmonic of a 20-kHz audio signal to be included in the measurement. Filter response is down 70 dB at 500 kHz, however, preventing feedthrough of RF carriers that are near the low end of the broadcast band.

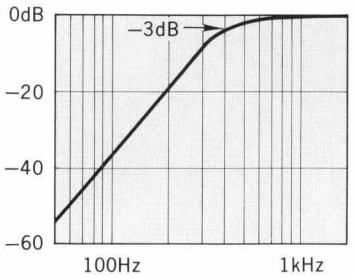

Fig. 9. *Switchable high-pass filter attenuates power line hum more than 40 dB. 3-dB cut-off point is at 400 Hz.*

BATTERY OPERATION

Terminals on the rear panel connect to the power supply regulators within the new analyzer, permitting the instrument to be operated from batteries where it is desired to eliminate ground loops arising from power-line interconnects. Two batteries are required, each within a voltage range of 28 to 50 volts, and each capable of supplying 80 mA.

The switched high-pass filter in the Automatic Nulling Distortion Analyzer removes any ac pickup that may

[2] Charles R. Moore, 'Two Ways to Measure Distortion,' **Electronics**, Vol. 38, No. 20, Oct. 4, 1965.

TABLE I. DISTORTION INTRODUCED BY RF DETECTOR

Frequency	550 - 1500 kHz		65 MHz	
Carrier level	1 V	3 - 8 V	1 V	3 - 8 V
THD at 30% modulation	– 48 dB	– 58 dB	– 38 dB	– 46 dB
THD at 100% modulation	– 28 dB	– 44 dB	– 25 dB	– 33 dB

TABLE II. INPUT IMPEDANCE OF RF DETECTOR

Frequency (MHz)	INPUT IMPEDANCE	
	Real component (ohms)	Reactive component (pF)
1	1.6 k	20
5	450	20
10	1.9 k	16
25	1.1 k	13
50	300	21

interfere with the measurement. As shown in the diagram of Fig. 9, the filter has a 3-dB point at 400 Hz and an 18 dB per octave roll-off. It attenuates 60-Hz hum components by more than 46 dB.

ACKNOWLEDGMENTS

The automatic nulling circuitry was developed by Larry A. Whatley and the broadband metering circuitry by Terry E. Tuttle. Product design was by Kay Danielson and Darrel Coble while overall electrical design was the responsibility of the undersigned. Many valuable ideas and suggestions were provided by Marco Negrete. The development was performed in the –hp– Loveland Laboratories.

—Charles R. Moore

SPECIFICATIONS -hp- MODELS 331A, 332A, 333A, AND 334A DISTORTION ANALYZERS

DISTORTION MEASUREMENT RANGE: Any fundamental frequency, 5 Hz to 600 kHz. Distortion levels of 0.1% - 100% full scale are measured in 7 ranges.

DISTORTION MEASUREMENT ACCURACY:
Harmonic measurement accuracy:

For fundamental of less than 30 V at input:

RANGE	Maximum Error		
	± 3%	± 6%	± 12%
100% - 0.3%	10 Hz - 1 MHz	10 Hz - 3 MHz	
0.1%	30 Hz - 300 kHz	20 Hz - 500 kHz	10 Hz - 1.2 MHz

For fundamental of more than 30 V at input:

RANGE	Maximum Error		
	± 3%	± 6%	± 12%
100% - 0.3%	10 Hz - 300 kHz	10 Hz - 500 kHz	10 Hz - 3 MHz
0.1%	30 Hz - 300 kHz	20 Hz - 500 kHz	10 Hz - 1.2 MHz

Elimination characteristics:
Fundamental rejection: >80 dB
Second harmonic accuracy for a fundamental of:
5 to 20 Hz: better than ± 1 dB
20 Hz to 20 kHz: better than ± 0.6 dB
20 to 100 kHz: better than – 1 dB
100 to 300 kHz: better than – 2 dB
300 to 600 kHz: better than – 3 dB

Distortion introduced by instrument:
< 0.03% from 5 Hz to 200 kHz
< 0.06% from 200 to 600 kHz

Meter indication: proportional to average value of sine wave.

FREQUENCY CALIBRATION ACCURACY:
Models 331A and 332A:
Better than ± 2% from 10 Hz to 200 kHz
Better than – 3% from 5 to 10 Hz
Better than + 8% from 200 to 600 kHz
Models 333A and 334A:
Better than ± 3% from 5 Hz to 200 kHz
Better than +8% from 200 to 600 kHz

INPUT LEVEL FOR DISTORTION MEASUREMENTS: 0.3 V rms for 100% Set Level or 0.245 V for 0 dB Set Level (up to 300 V may be attenuated to set level reference).

VOLTMETER RANGE: 300 μV to 300 V rms full scale (13 ranges) 10 dB per range.

VOLTMETER ACCURACY (using front panel input terminals):

VM RANGE	Maximum Error	
	± 2%	± 5%
300 μV	30 Hz - 300 kHz	20 Hz - 500 kHz
1 mV - 30 V	10 Hz - 1 MHz	5 Hz - 3 MHz
100 V - 300 V	10 Hz - 300 kHz	5 Hz - 500 kHz

NOISE MEASUREMENTS: Voltmeter residual noise on 300 μV range: < 25 μV rms, when input is terminated in 600 ohms. < 30 μV rms when terminated with shielded 100 k resistor.

INPUT IMPEDANCE:
Distortion Mode: 1 Megohm shunted by less than 60 pF (10 megohms shunted by < 10 pF with -hp- 10001A Divider Probe).
Voltmeter Mode: 1 Megohm shunted by 30 pF, 1 to 300 V rms; 1 Megohm shunted by 60 pF, 300 μV to 0.3 V rms.
(Input capacitance increased 20 pF with rear input modification.)

DC ISOLATION: Signal ground may be ± 400 Vdc from external chassis.

OUTPUT: Approximately 0.1 V rms output for full scale meter deflection.

OUTPUT IMPEDANCE: 2 kilohms.

AUTOMATIC NULLING MODE
(Models 333A and 334A)

SET LEVEL: at least 0.2 V rms.

HOLD-IN CHARACTERISTICS:
×1 frequency range-manual null tuned to less than 3% of set level; total frequency hold-in ±0.5% about true manual null. × 10 through ×10k frequency ranges-manual null tuned to less than 10% of set level; total frequency hold-in ±1% about true manual null.

AUTOMATIC NULL ACCURACY:
5 to 100 Hz: Meter reading within 0 to + 3 dB of manual null. 100 Hz to 600 kHz: Meter reading within 0 to + 1.5 dB of manual null.

HIGH-PASS FILTER: 3-dB point at 400 Hz with 18-dB-per-octave roll-off. 60-Hz rejection > 40 dB. Normally used only with fundamental frequencies greater than 1 kHz.

AM DETECTOR
(Models 332A and 334A)

DETECTOR: High impedance dc-restoring peak detector with semiconductor diode operates from 550 kHz to greater than 65 MHz. Broadband input, no tuning required.

MAXIMUM INPUT: 40 V p-p or 40 V peak transient.

DISTORTION INTRODUCED BY DETECTOR (for 3 - 8 V rms carriers modulated 30%):
Carrier frequency 550 kHz - 1.6 MHz: <0.3%
Carrier frequency 1.6 - 65 MHz: <1%
NOTE: Distortion introduced at carrier levels as low as 1 volt modulated 30% normally is < 1% 550 kHz to 65 MHz.

GENERAL (All models)

POWER SUPPLY: 115 or 230 volts ± 10%, 50 to 1000 Hz, approximately 4 watts. Terminals are provided for external battery supply. Positive or negative voltages between 30 V and 50 V required. Current drain from each supply is 40 mA (Models 331A and 332A) or 80 mA (Models 333A and 334A).

SIZE: Nominally 16¾ in. wide by 5¼ in. high by 11¼ in. deep behind front panel.

WEIGHT: Net 17¾ lbs. (7,98 kg). Shipping 23 lbs. (10,35 kg).

PRICE: Model 331A: $590.00
Model 332A: $620.00
Model 333A: $760.00
Model 334A: $790.00
Option: 01, Indicating meter has VU characteristics conforming to FCC requirements for AM/FM and TV broadcasting: $15.00.

C10-331A, C10-332A, C10-333A, C10-334A, Rear input terminals in parallel with front terminals; price on request.

Prices f.o.b. factory
Data subject to change without notice

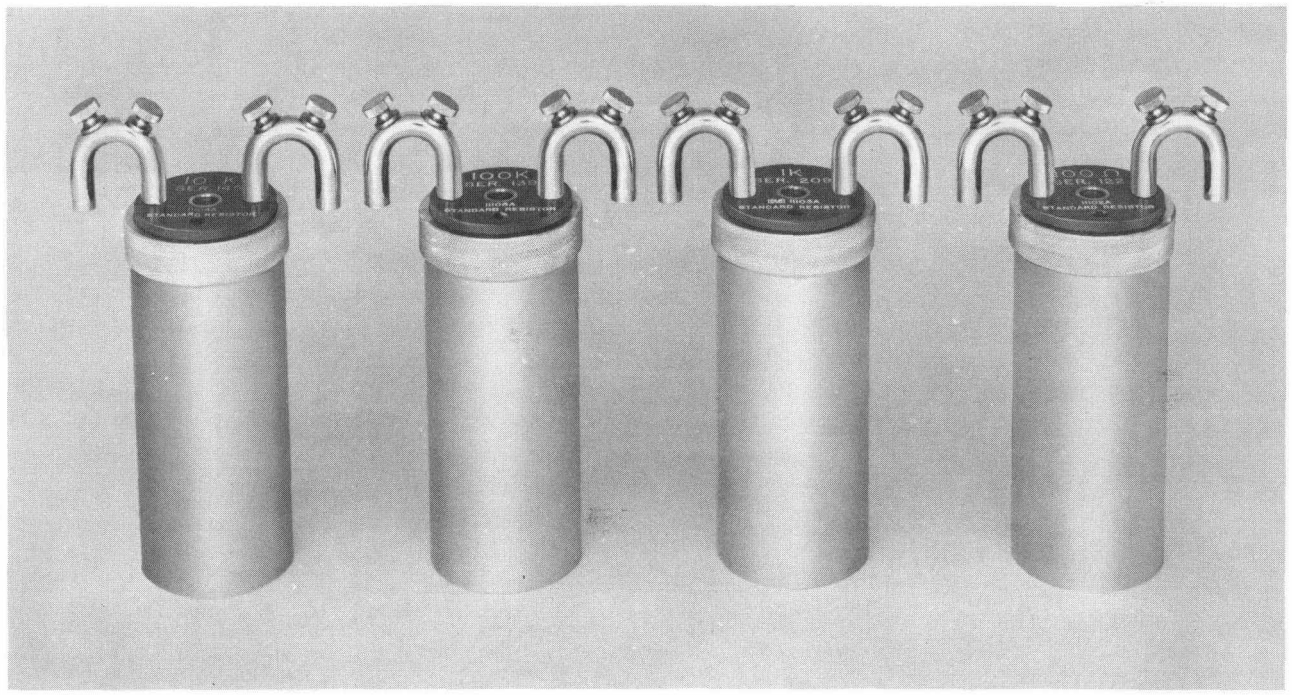

AN ADJUSTABLE STANDARD RESISTOR WITH IMPROVED ACCURACY AND HIGH STABILITY

A new standard resistor designed in the -hp- Standards Laboratory can be set to within ±0.15 ppm of nominal, substantially facilitating precision calibration work.

STANDARD RESISTORS are used in standards laboratories, calibration laboratories, and production areas for precision resistance measurements and precision voltage dividers, and for calibrating precision resistance-measuring and voltage-ratio devices. In most standards laboratories, the working standard for resistance measurements is the National Bureau of Standard (NBS) type of standard resistor, developed by E. B. Rosa and described by him in 1908.* The remarkably long tenure of this resistor and the many thousands now in use show that it has been a very satisfactory standard for most applications. But, like any other design, the Rosa type is less than perfect, and in the standards laboratories the need for an improved resistance standard has been recognized for many years.

A new type of standard resistor has now been developed in the Hewlett-Packard Palo Alto Standards Laboratory. The new standards are adjustable with a precision of a small fraction of 1 part per million (0.0001%), and are set at the factory to be within 1 part per million (ppm) of their nominal resistance values, in terms of standards calibrated by the National Bureau of Standards. (An uncertainty in the NBS calibration gives an overall uncertainty of about ±6 ppm in the values of the new resistors.) Some Rosa-type resistors, on the other hand, may differ from their nominal resistance values by up to ±50 ppm (with similar uncertainties).

*This resistor is used by the National Bureau of Standards as a standard for resistance values greater than one ohm. The NBS standard 1-ohm resistor is the Thomas type, developed in 1931

The principal difference between the new resistors and older types is their adjustability. Accuracy requirements of 1 ppm or better are now common for resistance measurements and voltage dividers in standards laboratories. Since the resistance of a typical Rosa-type standard may differ from its nominal value by as much as ±50 parts per million (ppm), and no provision is made for subsequent adjustment, corrections must be applied whenever these resistors are used in applications requiring accuracies of the order of 1 ppm. The correction is different for each resistor, which means that considerable calculation may be required, especially when several standard resistors are involved, as they are, for example, in precision voltage dividers.

The new –*hp*– design, on the other hand, is much simpler to use. These resistors can be set to within 0.15 ppm of the desired resistance value. Nearly perfect voltage dividers can be synthesized by setting several resistors, say 10, equal to each other within ±0.15 ppm, and selecting an average one of the 10 for the bottom resistor of the divider. Provided that no temperature changes occur, the accuracy of the resulting ratio of 10 to 1 will be better than that of the individual resistors by an order of magnitude, i.e. ±0.015 ppm.[1] More important for the user, this accuracy can be obtained without calculations of any kind.

The new resistors are now available in nominal values of 100 ohms, 1 kilohm, 10 kilohms, and 100 kilohms. Additional values to be available in the near future will be 1 ohm, 10 ohms, and 1 megohm.

CONSTRUCTION

Both the –*hp*– resistor and the Rosa resistor are wire-wound resistors in which the resistance element is a coil of resistance wire supported by a cylindrical form. However, there are three major differences in construction. First, there is no brass form in the finished –*hp*– resistor, as there is in the Rosa-type; instead, the coil and two layers of polyester form a thin self-supporting shell. Second, the –*hp*– resistor is adjustable: a trimming potentiometer and associated resistance coils are added to the basic resistance coil to permit precise setting of the final value.

[1] 'Establishing Ratios to One Part in Ten Million,' 'JRL Precision,' Vol. IV, No. 1, June, 1961.

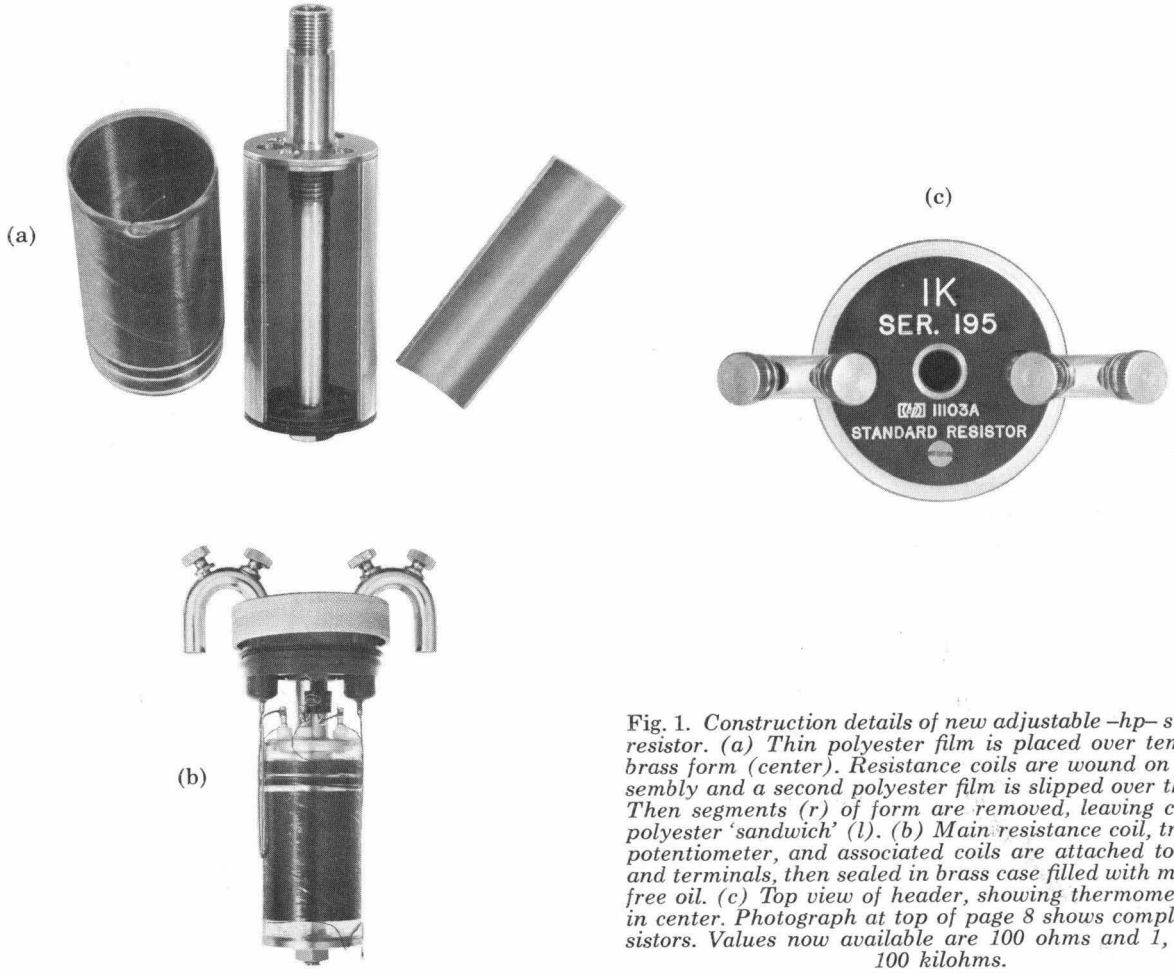

Fig. 1. *Construction details of new adjustable –hp– standard resistor. (a) Thin polyester film is placed over temporary brass form (center). Resistance coils are wound on this assembly and a second polyester film is slipped over the coils. Then segments (r) of form are removed, leaving coil-and-polyester 'sandwich' (l). (b) Main resistance coil, trimming potentiometer, and associated coils are attached to header and terminals, then sealed in brass case filled with moisture-free oil. (c) Top view of header, showing thermometer well in center. Photograph at top of page 8 shows completed resistors. Values now available are 100 ohms and 1, 10, and 100 kilohms.*

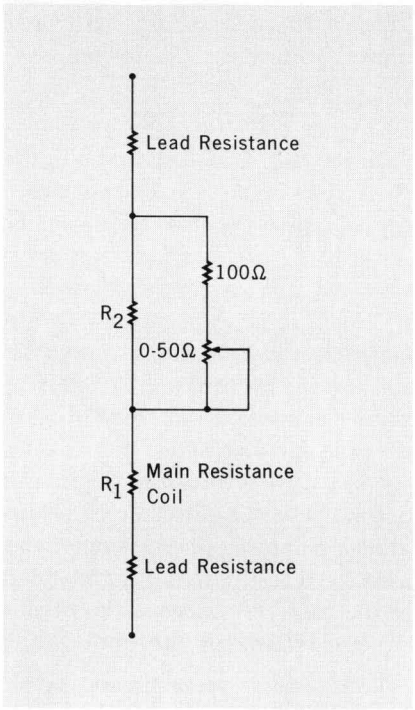

Fig. 2. *Circuit diagram of adjustable standard resistor.*

Third, the non-metallic materials used in the –*hp*– resistor are all modern plastics, which are considerably more inert than the phenolic, hard rubber, cotton, and silk used in the older resistors.

Fig. 1 is a series of views showing the construction of the new resistors. The completed resistors, hermetically sealed in their oil-filled brass cases, are shown in the photograph at the top of page 8.

The completed winding actually has several sections. Fig. 2 is a wiring diagram, showing the main coil R_1 in series with the additional coils and the 50-ohm potentiometer. The value of R_2 varies with R_1, so that the same 50-ohm pot gives a range of adjustability of about ±25 ppm for all resistance values.

SETTABILITY

The adjustability of the new standard resistors makes it possible to set one of them equal to a reference standard, or to set several of them equal to each other, with great precision. The precision with which they can be set is a function of the resolution of the wire-wound, 50-ohm trimming potentiometer. The minimum adjustment, or resolution, of this potentiometer is 0.2 to 0.3 ppm, which permits the resistor to be adjusted to within ±0.1 to 0.15 ppm of the nominal resistance.

The high-quality wire-wound potentiometer can be adjusted with a screwdriver to change the resistance of the standard by ±25 to ±30 ppm. Because the range of adjustability is small, the stability and thermal characteristics of the standard are not appreciably affected by the presence of the potentiometer. Access to the adjusting screw is guarded by a removable plug screw which can be sealed with lacquer if desired.

Settability of the –*hp*– standards is especially significant when precision voltage dividers are needed, as is often the case in standards laboratories. Precision dividers can be synthesized by a simple matching process, and can be used in normal operations without calculating any correction factors. To form a two-decade divider, ten resistors of the same nominal value can be matched to each other; then each of nine re-

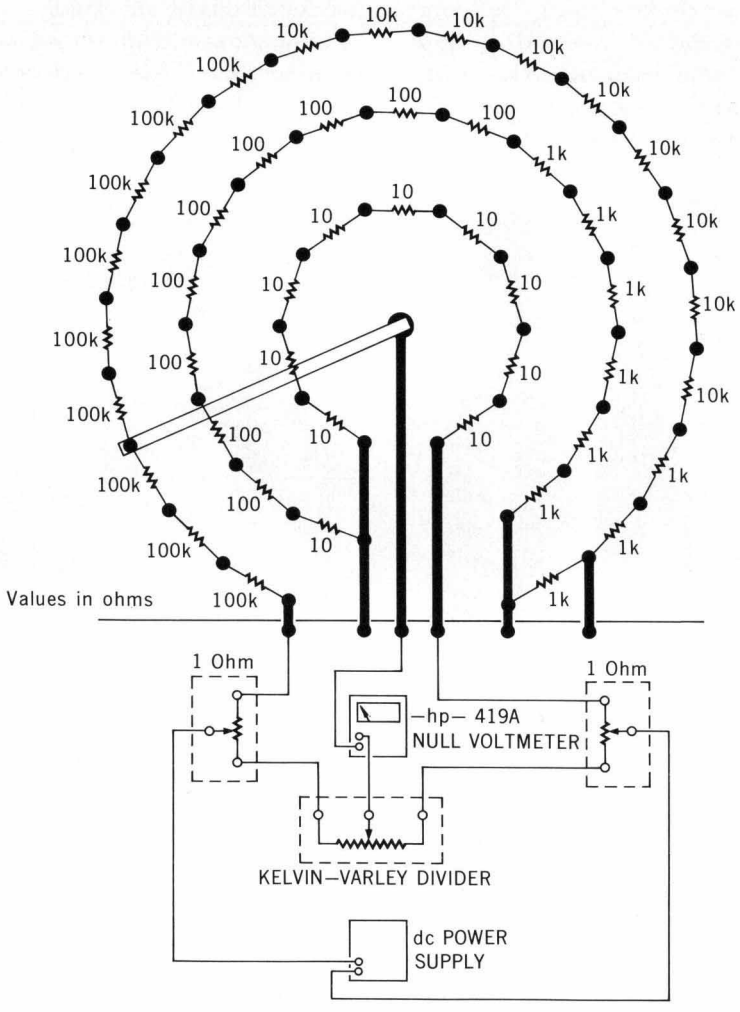

Fig. 3. *Schematic diagram of precision voltage divider shown on cover. Divider consists of 46 adjustable standard resistors in constant-temperature oil bath, and is used by –hp– Standards Laboratory to calibrate Kelvin-Varley voltage dividers and other precision instruments. Adjustability of resistors permits precise setting of ratios and eliminates many calculations.*

sistors of the next higher decade value can be matched to the sum of the first ten. This process can be carried further to make as many decades as desired.

The cover photograph shows a precision 5-decade divider designed and built in the –hp– Standard Laboratory. The divider consists of 46 resistors in a constant-temperature oil bath. This precision divider is used by the Standards Laboratory in calibrating universal ratio sets, volt boxes, and Kelvin-Varley voltage dividers, and in many other applications. Because of the physical arrangement and the adjustable standards, many operations which previously were tedious and time-consuming can now be performed quickly, accurately, and conveniently. (See Fig. 3 for a schematic diagram of the arrangement shown on the cover.)

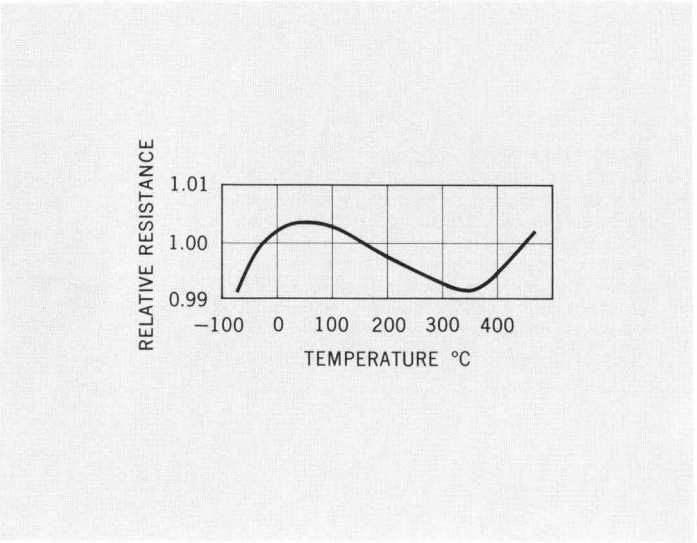

Fig. 4. *Variation of resistance of resistance wire with temperature.*

STABILITY

Stability of a resistor is the percentage change in its resistance over a specified period of time, usually one year. Stability data currently available for –hp– standard resistors are based upon 3 to 4-month tests of groups of 10 resistors, and indicate that the new resistors have maximum drifts of 5 to 8 ppm/year. Typical drifts are specified as 3 to 5 ppm/year, depending upon the resistance value. This compares favorably with older standards, which drift an average 8 ppm/year.[2]

Longer tests of larger numbers of resistors will be necessary before the long-term stability of the new standards is known with certainty. However, it is significant that the new resistors can be readjusted to compensate for drift, and this is not possible with older types.

THERMAL CHARACTERISTICS

The resistance of a wire-wound resistor is a function of the temperature of the wire. This temperature can change, either because of the self-heating which accompanies current flow in the wire, or because of variations in the ambient temperature.

Fig. 4 shows how the resistance of a typical sample of resistance wire varies with temperature. Notice the relatively flat portion of the curve near room temperature. For 15 or 20°C on either side of the center of this flat spot, the resistance can be described accurately by the formula

$$R_T = R_{25}[1+\alpha(T-25)+\beta(T-25)^2]$$

Where R_T is the resistance at T°C, R_{25} is the resistance at 25°C, and α and β are temperature coefficients which are determined experimentally for each resistor.

In the new –hp– standards, the wire is Evanohm (75% nickel, 20% chromium, 2.5% aluminum, 2.5% copper) with typical values of α between 0 and +2 ppm/°C. Evanohm wire has high resistivity and a relatively flat resistance-vs-temperature curve, and is stable and insensitive to moisture.

The temperature coefficients (α) of older standard resistors are typically 5 ppm/°C or higher. One of the reasons for this large α is that the brass form expands when its temperature rises, and this stresses the resistance wire and causes its resistivity to change. This problem is greatly reduced in the –hp– resistors. Wire stress is much smaller because the thin polyester form does not stress the wire, and because care is taken in the winding operation to minimize the tension on the wire and to avoid twisting or straining the wire. As a result, the effective temperature coefficients of the new resistors are very nearly those of the wire alone.

Fig. 5 shows resistance-vs-time curves for two types of standard resistors. Both were wound from the same wire, but on different forms. The tests were 34 minutes long, and the power level was 0.1 W, which is a common level for resistance measurements.

Fig. 5a is for a resistor with a brass form similar to that used in the Rosa-type. The apparent temperature coefficient α for this resistor was about +7 ppm/°C. Fig. 5b is for a resistor with a form consisting of one layer of polyester under the resistance wire and one over, like the form used in the new standard re-

[2] J. L. Thomas, 'Precision Resistors and Their Measurement,' National Bureau of Standards Circular 470, 1948, p. 10.

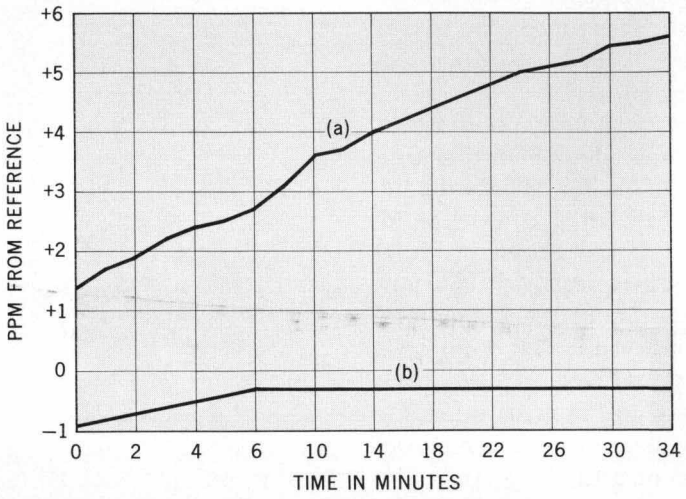

Fig. 5. *Changes in resistance values of standard resistors due to self-heating, showing effects of type of form on which coils are wound. (a) is for resistor with brass form, as in Rosa-type standard resistor. (b) is for polyester form, as in –hp– type. Both resistors were wound of same wire and power levels were both 0.1 W. (Note expanded time scale for first 6 minutes.)*

sistors. The coefficient α for this resistor was about +1.5 ppm/°C, very close to the temperature coefficient of the wire alone.

At a power level of 0.1 W, the new resistors reach thermal equilibrium in oil at a temperature which is about 0.5°C above their initial value. This results in a maximum resistance change of about 1 ppm.

Another thermal effect which can be troublesome in resistance measurements is the generation within the resistor of thermoelectric voltages due to junctions between dissimilar metals (e.g., Evanohm-copper). In the new resistors, careful attention has been given to eliminating these voltages by balancing them out.

TRANSIENT PERFORMANCE

When voltage is applied to a Wheatstone bridge circuit which contains a Rosa-type standard resistor in one of the arms, there is often a large swing of the galvanometer pointer, followed by a slow recovery towards a steady-state indication. A typical swing for a 10-kilohm resistor may be 10 to 50 ppm, with a recovery time of half a minute or more. The effect is smaller on 1-kilohm resistors and hardly noticeable for resistances of 100 ohms or less, but is larger for resistances greater than 10 kilohms.

Although this phenomenon is often called 'inductive kick,' standard resistors are usually wound so as to reduce inductive effects, and a 10-kilohm coil on a brass form acts more like a capacitance of 500 to 3300 pF. (The –hp– type, with its polyester form, has a capacitance of about 12 pF and an inductance of a few millihenries.) Charging of this large winding capacitance certainly contributes to the galvanometer swing. However, the time constant of the typical recovery towards null

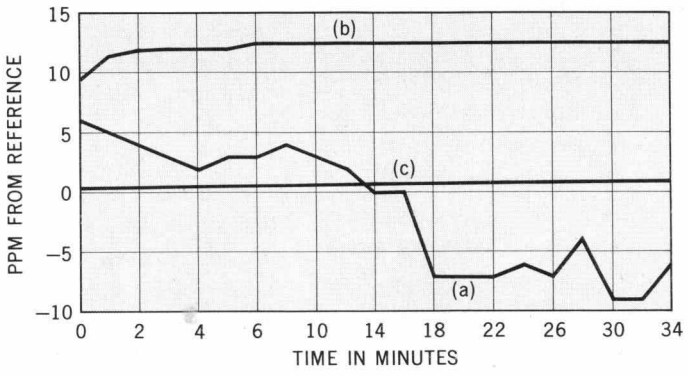

Fig. 6. *Changes in resistance values of standard resistors at power level of 0.1 W. (a) Rosa-type resistor before cleaning of header. (b) Same resistor after header was cleaned, showing that many transient effects are caused by electrochemical cell formed on header by impurities. (c) –hp– type (Serial No. 0018) after two years service, showing that contamination has been eliminated by use of inert materials. (Note expanded time scale for first 6 minutes.)*

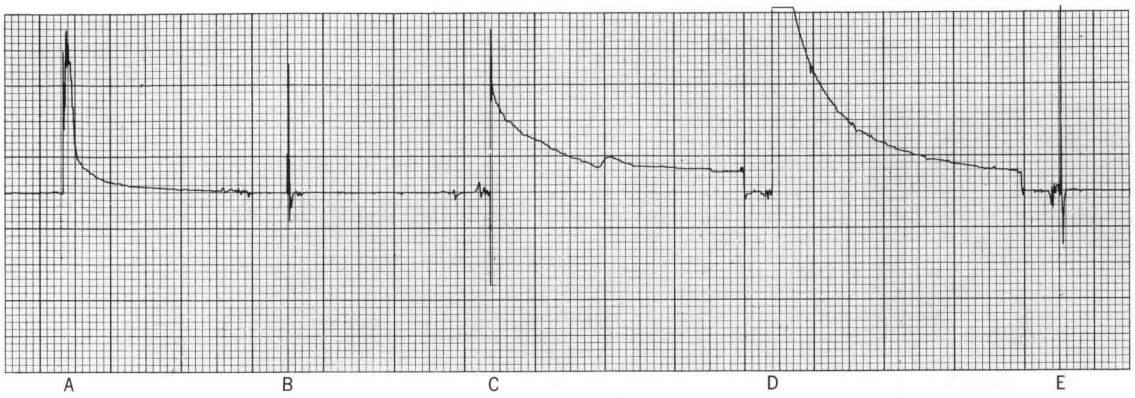

Fig. 7. *Typical recorder traces of transient voltages across headers of 5 standard resistors. With resistance coils disconnected, headers were charged to 30 V, then were allowed to discharge through 50 kilohms. Resistors A, C, D, E are Rosa-type; resistor B is –hp– type. Headers B and E show only capacitance-charging effects. Others show long-time-constant transient known as 'inductive kick'. Results show this is due to cell formed on phenolic headers by impurities, not to reactance of resistance coil. Vertical scale 2.5 μV per division, horizontal scale 2 in per min.*

is too long to be caused by the charging of even a 3300-pF capacitance.

Studies of this phenomenon which have been undertaken by the –hp– Standards Laboratory have led to the conclusion that its principal cause is the formation of a small cell, or battery, on the surface of the header in the older type of standard resistor. Chemical analysis of scrapings from phenolic headers which have been in use for several years has shown that the scrapings contain relatively large amounts of calcium, silicon, magnesium, lead, and iron. The electrochemical cell formed on the header by such substances can cause almost unpredictable transient effects.

Fig. 6 shows the performance of two standard resistors in 34-minute tests. Curve (a) is for a typical Rosa standard which had been in service for a number of years. Curve (b) is for the same resistor after the header had been scrubbed. The erratic behavior of curve (a) was greatly reduced by cleaning the header, indicating that chemical deposits are indeed responsible for some of the transient behavior of older standard resistors. The resistor used in this test began to behave erratically again about six months after it was cleaned, and a second cleaning again restored its stability.

To eliminate the contaminants that were present in older types, the non-metallic parts of the new resistors are made of modern plastics which are chemically inert. Polycarbonate, nylon, and polyester are used as structural elements, and formvar insulation is used on all metal parts so that none of the resistor circuitry is in contact with the oil.

Curve (c) of Fig. 6 is for a typical –hp– standard resistor which had been in service for about two years. In contrast to the older type, it showed no erratic behavior at all.

The theory that 'inductive kick' is caused by the formation of a small cell on the header was further verified by the results of tests involving the headers alone. The headers of several 10-kilohm standard resistors, both Rosa-type and –hp– type, were disconnected from their resistance coils and charged for several minutes with 30 volts between their terminals. The headers were then carefully transferred to the input

PAUL HUBBS

Paul Hubbs joined –hp– in 1952 as a microwave development engineer. He moved to the -hp- Standards Laboratory when it was established in 1953, and he is now responsible for dc and low-frequency standards in the Corporate Standards Laboratory in Palo Alto. He was responsible for the design of the Model 738AR VTVM Calibration System and has designed many special-purpose instruments.

From 1941 to 1950, Paul was a radio station manager in Portuguese Macao and a flight crew member for an international airline firm.

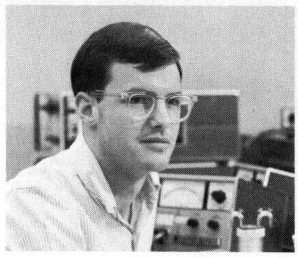

HENRY T. HETZEL

Henry Hetzel graduated from Haverford College in 1961 with a B.S. degree in Physics. After a year of graduate study at the University of Pennsylvania, he worked for one year on instruments for the blind, and for two years as a designer of biomedical instrumentation.

Henry joined the –hp– Loveland Division in 1965, and is now in charge of production of the new standard resistors. He is also continuing his work towards a Master's degree at Colorado State University.

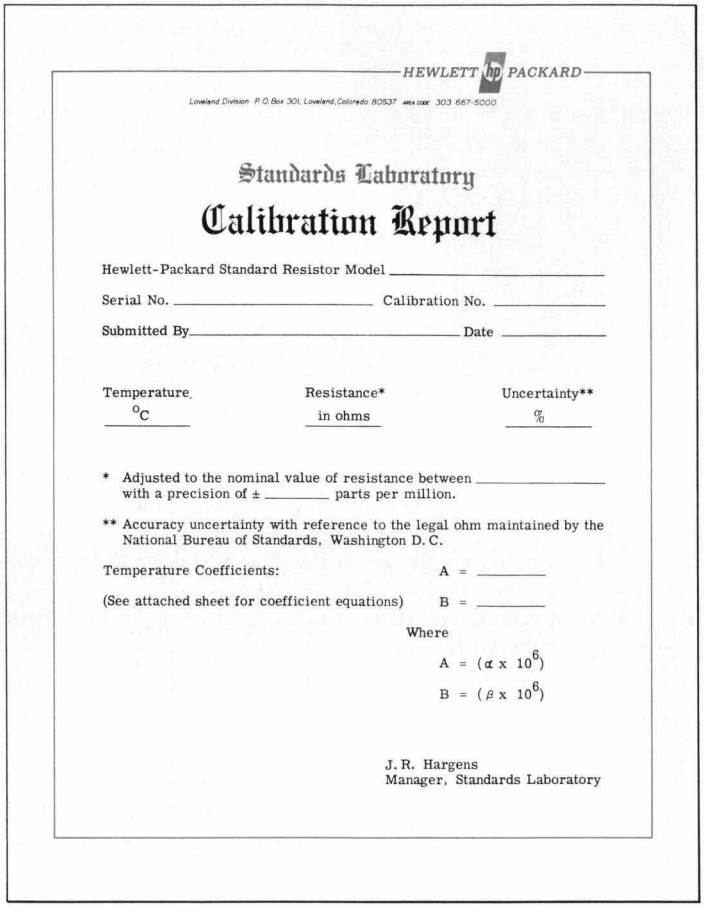

HEWLETT hp PACKARD

Loveland Division P.O. Box 301, Loveland, Colorado 80537 area code 303 667-5000

Standards Laboratory

Calibration Report

Hewlett-Packard Standard Resistor Model _____

Serial No. _____ Calibration No. _____

Submitted By _____ Date _____

Temperature °C	Resistance* in ohms	Uncertainty** %

* Adjusted to the nominal value of resistance between _____ with a precision of ± _____ parts per million.

** Accuracy uncertainty with reference to the legal ohm maintained by the National Bureau of Standards, Washington D. C.

Temperature Coefficients: A = _____

(See attached sheet for coefficient equations) B = _____

Where

$A = (\alpha \times 10^6)$

$B = (\beta \times 10^6)$

J. R. Hargens
Manager, Standards Laboratory

Fig. 8. *Calibration report is supplied with each standard resistor.*

terminals of a dc null voltmeter, and the meter readings were recorded on a strip-chart recorder. The effective resistance in parallel with the headers was 50 kilohms.

Fig. 7 shows typical recorder traces. The initial impulses were caused by the discharge of the header capacitances, which are a few picofarads with the resistance coils disconnected. After the initial impulses, the voltages across most of the headers decayed slowly towards zero. The curves are roughly exponential, and have time constants of half a minute or more. This is the behavior known as 'inductive kick.' This test shows that it is a property of the header and not of the resistance coils, and that it can more properly be called a 'cell effect.'

CALIBRATION REPORT

A calibration report (Fig. 8) is supplied with each resistor, certifying that it was set to its nominal value with a maximum uncertainty of ±6 ppm. Accuracy of this adjustment is traceable to the National Bureau of Standards. The calibration report also gives the temperature coefficients for each resistor, and a self-heating curve (not shown), which is a temperature-vs-time curve for the appropriate resistance value at a power level of 0.1 W.

ACKNOWLEDGMENTS

The adjustable standard resistor was designed by the author in the –hp– Standards Laboratory in Palo Alto. Other contributors to the project were John M. Hoyte, Glenn W. Weberg, Leslie C. Vickery, and B. P. Hand, head of the Standards Laboratory. Production design and manufacture are under the direction of Jack R. Hargens and Henry T. Hetzel of the –hp– Loveland Division. —*E. Paul Hubbs*

EMITTER FOLLOWER STABILITY *(cont'd from back cover)*

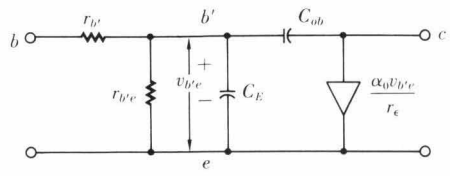

Fig. 3. *A more useful transistor equivalent circuit, valid for frequencies*

$$\omega \leqq \frac{\omega_T}{3}$$

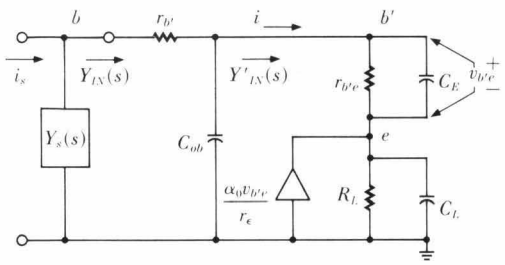

Fig. 4. *Equivalent circuit for circuit shown in Fig. 1.*

Substituting Z_E and Z_L into Equation 1 and rearranging gives

$$Y'_{IN}(s) = \frac{1}{(\beta_o + 1)\ (r_\epsilon + R_L)} \cdot \frac{r_{b'e}R_LC_EC_Ls^2 + (r_{b'e}C_E + R_LC_L)\ s + 1}{\frac{r_\epsilon R_L}{r_\epsilon + R_L}\ (C_L + C_E)\ s + 1} \quad (2)$$

The numerator and denominator polynomials can be separated into even and odd parts such that[2]

$$Y'_{IN}(s) = \frac{m_1(s) + n_1(s)}{m_2(s) + n_2(s)} \quad (3)$$

The even part of $Y'_{IN}(s)$ is given by

$$Ev\ Y'_{IN}(s) = \frac{m_1 m_2 - n_1 n_2}{m_2^2 - n_2^2} \quad (4)$$

with the real part resulting when $s = j\omega$. Thus

$$Re\ Y'_{IN}(j\omega) = Ev\ Y'_{IN}(s)\Big|_{s=j\omega} \quad (5)$$

Using Equations 2 through 5, the real part of the driving-point admittance can be found to be

$$Re\ Y'_{IN}(j\omega) = \frac{1}{(\beta_0 + 1)\ (r_\epsilon + R_L)} \cdot \frac{1 - \omega^2\left[r_{b'e}R_LC_EC_L - \frac{r_\epsilon R_L}{r_\epsilon + R_L}\left(C_L + C_E\right)\left(r_{b'e}C_E + R_LC_L\right)\right]}{1 + \omega^2\left[\frac{r_\epsilon R_L}{r_\epsilon + R_L}\left(C_L + C_E\right)\right]^2} \quad (6)$$

For the case where the imaginary part of the source impedance $Im\ Y_s(j\omega)$ is inductive, self-sustained oscillations will occur at a frequency determined by the source inductance and the transistor input capacitance for the condition

$$Re\ Y_s(j\omega) + Re\ Y'_{IN}(j\omega) \leqq 0 \quad (7)$$

Self-sustained oscillations will not exist so long as

$$Re\ Y_s(j\omega) + Re\ Y'_{IN}(j\omega) > 0 \quad (8)$$

Therefore, oscillations can be prevented by controlling either $Re\ Y_S(j\omega)$ or $Re\ Y'_{IN}(j\omega)$, or both.

If $Re\ Y_S(j\omega) > 0$, as is usually the case, stability can be assured by making $Re\ Y'_{IN}(j\omega) > 0$. From Equation 6 it can be determined that $Re\ Y_{IN}(j\omega) > 0$ so long as

$$r_{b'e}R_LC_EC_L < \frac{r_\epsilon R_L}{r_\epsilon + R_L}\ (C_L + C_E)\ (r_{b'e}C_E + R_LC_L) \quad (9)$$

or

$$r_\epsilon > \frac{\beta_0 r_\epsilon C_E}{C_L} - \frac{(\beta_0 + 1)\ r_\epsilon^2 C_E^2}{C_L^2 R_L} \quad (10)$$

where $r_\epsilon C_E$ = constant. For

$$\omega_T \cong \frac{1}{r_\epsilon C_E},$$

Equation 10 can be rewritten as

$$r_\epsilon > \frac{\beta_0}{\omega_T C_L} - \frac{\beta_0 + 1}{\omega_T^2 C_L^2 R_L} \quad (11)$$

DESIGN FOR STABILITY

Equation 10 or 11 represents a very useful design criterion for assuring the stability of a capacitively-loaded emitter follower with an inductive source. The dynamic emitter resistance r_ϵ is inversely proportional to the dc emitter current I_E:

$$r_\epsilon = \frac{kT}{q\,I_E}$$

where k is the Boltzmann constant, T is the absolute temperature, and q is the electronic charge. At room temperature,

$$r_\epsilon = \frac{0.026}{I_E}.$$

This means that Equation 10 or 11, and therefore the condition $Re\ Y'_{IN}(j\omega) > 0$, can be satisfied simply by adjusting the dc emitter current I_E. However, if the emitter current needed to meet this condition is contradictory to other design conditions (e.g., ac signal requirements), then the more general case given by Equation 8 should be considered.

—Glenn B. DeBella

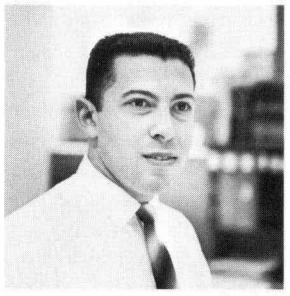

GLENN B. DeBELLA

Glenn DeBella joined –hp– in 1965 as a development engineer in the Frequency and Time Division. He has participated in the development of the 5260A Frequency Divider, and has given a series of lectures on transistors and linear circuits for engineers of the F and T Division.

Glenn holds BSEE and MSEE degrees from San Jose State College, and is a member of IEEE and Phi Kappa Phi. Before joining –hp–, he worked for three years as a circuit design engineer on magnetic tape recording equipment. He has also served for two years with the U.S. Army as a radar and radio technician.

[2] M. E. Van Valkenburg, "Introduction to Modern Network Synthesis", John Wiley & Sons, Inc., New York, 1960, Chapters 4 and 8.

STABILITY OF CAPACITIVELY-LOADED EMITTER FOLLOWERS—A SIMPLIFIED APPROACH

Emitter followers with a capacitive load often oscillate when driven from an inductive source. The following analysis shows that simple adjustment in bias current will often stabilize the circuit. The analysis is rigorous, yet provides a much simpler result than is known to have been published.

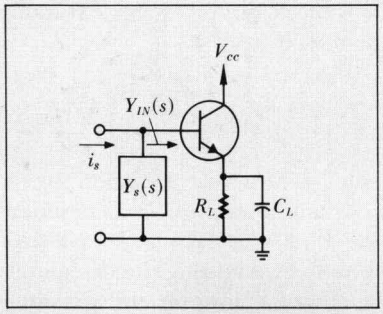

Fig. 1. *Emitter follower with a capacitive load.*

Common-collector transistor amplifiers, or emitter followers, are useful in electronic systems because they have both high input impedance and low output impedance. However, self-sustained oscillations may occur if the load on an emitter follower is capacitive and the impedance of the source which is driving the emitter follower is inductive.

In this article, stability criteria are derived which are useful in the design of capacitively-loaded emitter followers. The approach taken is that of examining the even or real part of the driving-point admittance and determining conditions for stable operation. Stability criteria for the capacitively-loaded emitter follower have, of course, been published before, but the analyses have not resulted in simple, easily-applied results. The following derivation is rigorous, yet gives a much more easily-applied result than is known to have been presented previously. The result shows, in fact, that a simple adjustment in dc emitter current can eliminate emitter-follower instability in many cases.

EQUIVALENT CIRCUIT

An emitter follower with a capacitive load is shown schematically in Fig. 1. Fig. 2 shows a very complete equivalent circuit for the transistor.

Fig. 3 is a transistor equivalent circuit which is valid for frequencies up to $\omega_T/3$, where ω_T is the transistor short-circuit current gain-bandwidth product in the common-emitter configuration. This circuit is a good compromise between simplicity and accuracy, and is adequate for most design work.[1]

Using the transistor equivalent circuit of Fig. 3, the circuit of Fig. 1 reduces to that shown in Fig. 4.

EMITTER FOLLOWER STABILITY

Conditions for the stability of the circuit of Fig. 4 can be found by examining the real part of the driving-point admittance $Y_{IN}(s)$. For this analysis the transverse base resistance $r_{b'}$ can be neglected, so the real part of $Y_{IN}(s)$ can be considered to be the same as the real part of the admittance $Y'_{IN}(s)$ in Fig. 4.

Solving for $Y'_{IN}(s)$ gives

$$Y'_{IN}(s) = \frac{i(s)}{v_{b'}(s)} = \frac{1}{Z_E + Z_L\left(1 + \frac{\alpha_0 Z_E}{r_\epsilon}\right)} \qquad (1)$$

where $$Z_E = \frac{r_{b'e}}{r_{b'e}C_E s + 1}$$

and $$Z_L = \frac{R_L}{R_L C_L s + 1}$$

(concluded inside on p. 15)

[1] For a thorough discussion of transistor equivalent circuits, see M. S. Ghausi, "Principles and Design of Linear Active Circuits," McGraw-Hill Book Co., Inc., New York, N.Y., 1965.

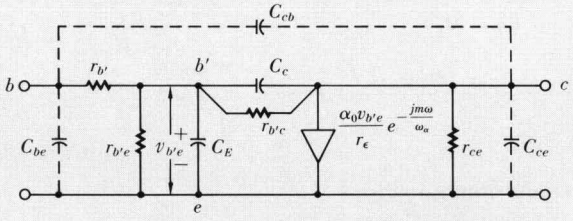

Fig. 2. *Transistor hybrid-pi equivalent circuit.*

$r_{b'c}$, r_{ce} — account for base-width modulation effects

$r_{b'}$ — transverse base resistance

r_ϵ — dynamic emitter resistance

$r_{b'e} = \frac{r_\epsilon}{1-\alpha_0} = r_\epsilon(\beta_0 + 1)$

α_0 — low frequency transistor current transfer ratio for common base configuration

β_0 — low frequency transistor current transfer ratio for common emitter configuration

C_{be}, C_{cb}, C_{ce} — header capacitances

C_c — collector-base junction capacitance

$C_E \cong \frac{1}{\omega_T r_\epsilon} - C_{ob}$

ω_T — transistor short-circuit current gain-bandwidth product in common emitter configuration

$C_{ob} \cong C_c + C_{cb} + C_{ce}$

$e^{-\frac{jm\omega}{\omega_\alpha}}$ — excess phase shift factor